LOWPASS LUMPED-ELEMENT COPLANAR WAVEGUIDE-TO-COPLANAR STRIPLINE TRANSITIONS

Yo-Shen Lin[1] and Chun Hsiung Chen[2]

[1]*Department of Electrical Engineering, National Central University, Chungli 320, Taiwan, R.O.C. (email: yslin@ee.ncu.edu.tw)*
[2]*Department of Electrical Engineering and Graduate Institute of Communication Engineering, National Taiwan University, Taipei 106, Taiwan, R.O.C. (email: chchen@ew.ee.ntu.edu.tw)*

ABSTRACT

The lowpass coplanar waveguide-to-coplanar stripline transitions are proposed, using planar lumped-elements to realize the filter prototypes in the transition structures. The proposed transitions are very compact and can provide the combined functions of transition and filter. Simple equivalent-circuit models based on closed-form expressions are also established, from which the characteristics of various lowpass lumped-element transitions are investigated.

INTRODUCTION

Coplanar waveguide (CPW) and coplanar stripline (CPS) are widely used as building blocks in the design of uniplanar MMIC's [1]. To fully utilize the exclusive features of CPW and CPS, an effective interconnection between them is of crucial importance. This may allow the choice of different uniplanar line-based circuit elements in different parts of a system such that maximum circuit integration and optimal system performance may be accomplished.

Various CPW-to-CPS transitions have been developed [2]-[7]. Most of these conventional transitions have bandpass behaviors [2]-[4]. The broadband transition [5] utilizing a slotline open structure has a lowpass frequency response but its insertion loss increases only gradually as the operating frequency increases. The ideally all-pass double-Y junction balun [2], in practice, also features a gradually increasing insertion loss with frequency.

In practical MMIC design, since the desired signal is always band-limited, a subsequent filter after the transition is usually required to filter out the unwanted spurious responses and harmonics. If the transition can be designed such that it exhibits the desired filter response, it will have the advantage of saving one additional filter as well as reducing the circuit area. In [6], the 3rd-order lumped-element CPW-to-CPS transitions with lowpass and highpass frequency responses were proposed, but the stopband characteristics were not clearly revealed due to the adoption of back-to-back configuration for transition measurement. A 2nd-order lowpass transition was also proposed in [7], but its stopband rejection is not good.

In this study, based on the measurement circuit suggested in [7], the stopband characteristic of the 3rd-order lowpass lumped-element transition in [6] is thoroughly investigated, and a better equivalent-circuit model is proposed. A method for post-fabrication tuning of the notch in the stopband is also introduced, such that more precise control of the transition frequency response is achievable. In addition, a novel elliptic lowpass transition is proposed to provide better stopband rejection, together with its equivalent-circuit model as effective design tool.

LOWPASS TRANSITION STRUCTURES

Consider the lowpass CPW-to-CPS transition proposed in [6] and shown in Fig. 1(a), which is equivalent to a T-type 3rd-order lowpass filter. Here the series inductors L_{s1} and L_{s2} in the filter prototype are realized by metal strips, and the shunt capacitor C_{p1} to ground is formed by the interdigital capacitor. The equivalent-circuit model based on closed-form expressions for this lowpass transition [Fig. 1(a)] is obtained by modifying that in [6], and is shown in Fig. 1(b). Here a six-port equivalent-circuit model [8]-[9] is adopted in order to take into account the mode conversion effect at the CPW-CPS cross-junction. In this model, the CPW line is represented by two transmission lines that separately support even CPW mode and odd CPW mode. Compared to the equivalent-circuit model in [6], here the metal strip inductor L_{s1} is modeled as a short-ended transmission line that supports the even CPW mode instead of a lumped inductor. This modification may better describe its high frequency behavior when its length reaches a quarter-wavelength ($\lambda/4$).

A lowpass transition for Fig. 1(a) is built on an FR4 substrate ($\varepsilon_r = 4.3$, $\tan\delta = 0.022$, and thickness h = 1.6 mm), and for measurement purposes, its CPS port is alternatively connected to that of a broadband transition [5] as suggested in

TABLE I. GEOMETRICAL PARAMETERS OF THE LOWPASS CPW-TO-CPS TRANSITIONS (UNITS IN mm)

Fig.	Interdigital Capacitor					Inductor		
		Finger Number	Finger Length	Finger Width	Gap Width		Strip Length	Strip Width
Fig. 2	C_{p1}	5	4.1	0.6	0.2	L_{s1}	8.6	0.2
						L_{s2}	8.5	0.3
Fig. 5	C_{p1}	5	2	0.5	0.2	L_{s1}	8.2	0.2
	C_{s2}	5	3.1	0.5	0.2	L_{s2}	4.9	0.2

[7]. Compared to the back-to-back configuration in [6], one may better examine the frequency response of a single lowpass transition based on this test circuit. In this and subsequent designs, the CPW lines have a strip width of 0.45 mm, a slot width of 0.6 mm, and a finite ground-plane width of 4 mm. The CPS lines have a strip width of 4 mm and a slot width of 0.6 mm. Both CPW and CPS lines are designed to possess a characteristic impedance of 100 Ω according to [1]. The designed element values are L_{s1} = 8.2 nH, C_{p1} = 0.92 pF, and L_{s2} = 7.5 nH. Their corresponding geometrical parameters are listed in Table I.

The transition is measured on an HP8753 network analyzer with TRL (Thru-Reflect-Line) calibration to the CPW-CPS junction. The measured and simulated results are shown in Fig. 2. Here the simulation results obtained from the equivalent-circuit model [Fig. 1(b)] and the full-wave simulator HFSS are both included. Note that the frequency response of the lowpass transition is much different from that of the ideal 3rd-order filter prototype. This is due to the two additional notches introduced in its insertion loss response. The first notch at 2.93 GHz is due to the series resonance of capacitor C_{p1} with the bondwire inductances. The other notch at 4.6 GHz occurs when the length of metal strip inductor L_{s1} reaches λ/4 such that it is equivalent to an open circuit. These two additional notches improve the stopband rejection and the roll-off rate at passband edge. The measured insertion loss of proposed transition is less than 1.5 dB below 1.63 GHz, and the return loss is better than 15 dB below 1.55 GHz. The out-of-band rejection is greater than 20 dB from 2.66 GHz up to 5.04 GHz. The agreement between measured results and simulated ones from the equivalent-circuit model [Fig. 1(b)] is good at low frequencies. At higher frequencies, the metal strip inductor and interdigital capacitor can no longer be considered as lumped-elements, and the parasitic effects, which are not included in the equivalent-circuit model, start to dominate. Thus the discrepancy between measurement and equivalent-circuit model is larger. The simulated results from HFSS match well with the measured ones. However, the simulation time is several hours for HFSS while it takes only a few seconds for the equivalent-circuit model. Nevertheless, the equivalent-circuit model may serve as a better tool for transition prototype design because all the elements in the model are directly related to the geometrical parameters of transition. The full-wave simulation may then be employed for better accuracy.

The lowpass transition also supports post-fabrication tuning of the notch frequency. As stated above, the first notch in the stopband is due to the series resonance of C_{p1} with bondwire inductances. Since the bondwire inductance is connected to the cross-junction through the transmission line for odd CPW mode in the equivalent-circuit model, increasing the length of this odd CPW mode transmission line may increase the effective inductance connected to C_{p1}

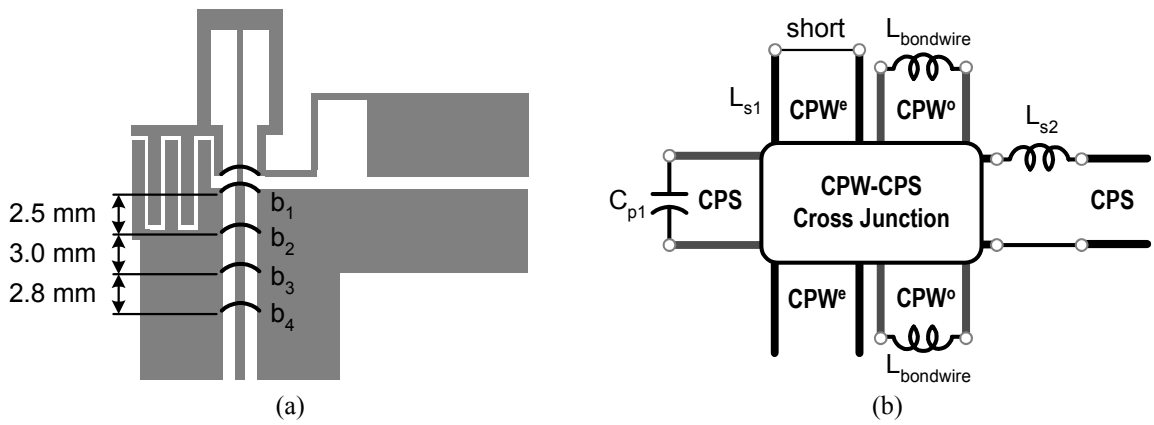

Fig. 1. 3rd-order lowpass CPW-to-CPS transition, (a) layout and (b) equivalent-circuit model.

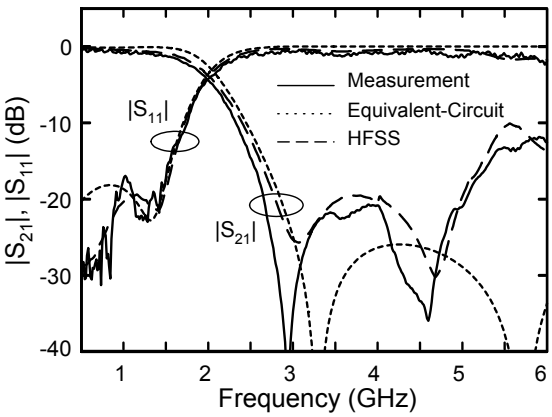

Fig. 2. Measured and simulated results for the 3rd-order lowpass CPW-to-CPS transition shown in Fig. 1(a).

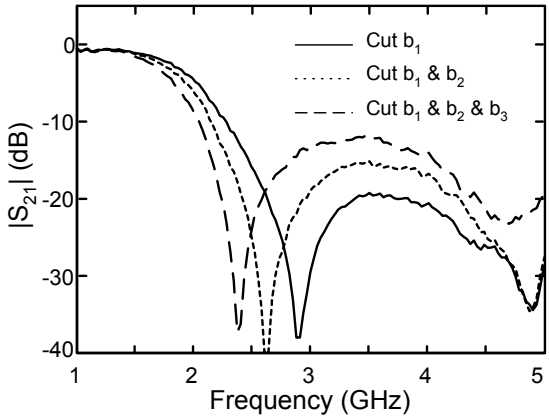

Fig. 3. Measured results for the 3rd-order lowpass CPW-to-CPS transition shown in Fig. 1(a) with the bondwires b_1, b_2, and b_3 being cut in turn.

and thus lower the notch frequency. Variation of the transmission line length for odd CPW mode may be accomplished by changing the location of bondwire. The transition structure in Fig. 1(a) is fabricated with four bondwires b_1 to b_4 along the CPW line each separated by about 3 mm. By removing the bondwires after transition fabrication, one may effectively increase the distance of the bondwire to the cross-junction. Fig. 3 shows the measured frequency responses after cutting the bondwires b_1, b_2, and b_3 in turn. With each removal of a bondwire, the notch frequency is lowered by about 250 MHz. This tuning capability may allow more tolerance in the transition fabrication and provide more precise control over the transition frequency response.

To further improve the stopband rejection of the transition, a 3rd-order elliptic lowpass filter prototype may be adopted. This is done by replacing the series inductors in the 3rd-order lowpass filter prototype by parallel LC circuits. The resulting transition structure is shown in Fig. 4(a) with its equivalent-circuit model in Fig. 4(b). In Fig. 4(a), an interdigital capacitor C_{s2} is added in parallel with L_{s2} to form one parallel LC circuit. The other is accomplished by the distributed effect of metal strip inductor L_{s1} when its length reaches $\lambda/4$, for its input impedance will then be similar to that of a parallel LC circuit. The resonant frequencies of these parallel LC circuits are designed to create additional notches at stopband to improve the level of attenuation.

A lowpass transition for Fig. 4(a) is built on an FR4 substrate with the test circuit built in the same way as in Fig. 2. The element values are: L_{s1} = 7.5 nH, C_{p1} = 0.55 pF, L_{s2} = 4 nH, and C_{s2} = 0.7 pF. Their corresponding geometrical parameters are listed in Table I. Measured and simulated results are shown in Fig. 5. The measured insertion loss is less than 1.5 dB below 2.06 GHz, and the return loss is better than 15 dB below 1.7 GHz. The out-of-band rejection is greater than 15 dB from 2.74 GHz up to 6 GHz. Compared to Fig. 2, the elliptic lowpass transition exhibits sharper roll-off at the passband edge, and better attenuation at higher frequencies. This is due to the additional notch created by the resonance of L_{s2} with C_{s2} at 3 GHz. The notch at 4.7 GHz is caused by the resonance of C_{p1} with bondwires, while the one at 5.7 GHz is due to L_{s1} when its length reaches $\lambda/4$. Therefore, by properly choosing the notch frequencies

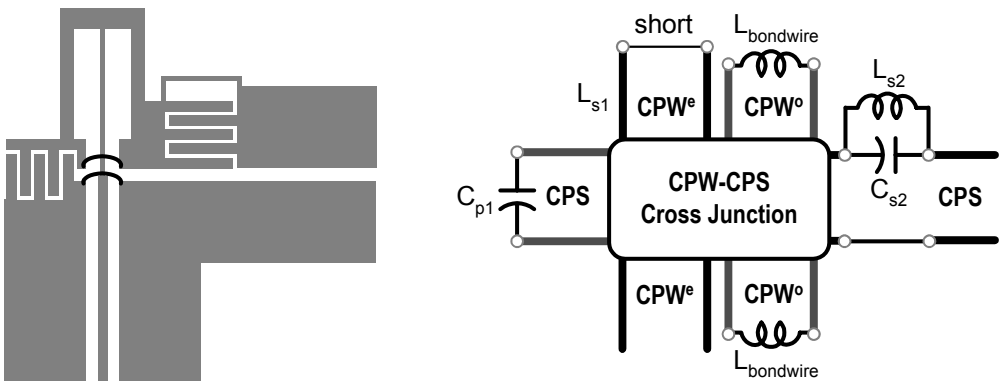

(a) (b)

Fig. 4. 3rd-order elliptic lowpass CPW-to-CPS transition, (a) layout and (b) equivalent-circuit model.

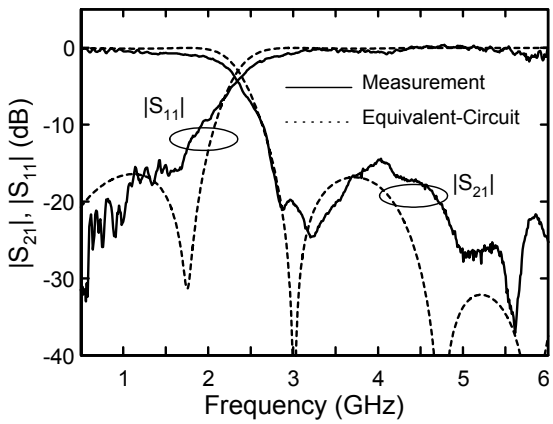

Fig. 5. Measured and simulated results for the 3rd-order elliptic lowpass CPW-to-CPS transition shown in Fig. 4(a).

through the adjustment of L and C values, one may achieve the design specification for stopband rejection.

CONCLUSIONS

In this study, the lowpass lumped-element CPW-to-CPS transitions have been proposed and carefully examined. The proposed lowpass transitions feature sharper roll-off rate and better stopband attenuation compared to the conventional ones. The junction parasitic effects introduce additional notches at stopband, such that the required attenuation may be accomplished with lower filter orders. The lowpass transitions also feature post-fabrication tuning of the notch frequency, such that more precise control over the transition frequency response may be accomplished. The proposed transitions are very compact, and can improve the harmonic attenuation and spurious rejection for applications like antenna feeding structures or balanced mixers. They may have the advantage of saving one additional filter or at least relaxing the requirements on subsequent filters, thus they are attractive for uniplanar MMIC applications.

ACKNOWLEDGMENT

This work was supported by the Ministry of Education and by the National Science Council of Taiwan under Grant 89-E-FA06-2-4 and Grant NSC 91-2219-E-002-016.

REFERENCES

[1] K. C. Gupta, R. Garg, I. J. Bahl, and P. Bhartia, *Microstrip Lines and Slotlines*, 2nd ed. Norwood, MA: Artech House, 1996, ch. 7.

[2] V. Trifunovic' and B. Jokanovic', "Review of printed Marchand and double Y baluns: characteristics and application," *IEEE Trans. Microwave Theory Tech.*, vol. 42, pp. 1454-1462, Aug. 1994.

[3] L. Zhu and K. Wu, "Hybrid FGCPW/CPS scheme in the building block design of low-cost uniplanar and multilayer circuit and antenna," in *IEEE MTT-S Int. Microwave Symp. Dig.*, pp.867-870, 1999.

[4] Y.-S. Lin and C. H. Chen, "Novel lumped-element uniplanar transitions," *IEEE Trans. Microwave Theory Tech.*, vol. 49, pp. 2322-2330, Dec. 2001.

[5] S.-G. Mao, C.-T. Hwang, R.-B. Wu, and C. H. Chen, "Analysis of coplanar waveguide-to-coplanar stripline transitions," *IEEE Trans. Microwave Theory Tech.*, vol. 48, pp. 23-29, Jan. 2000.

[6] Y.-S. Lin and C. H. Chen, "Novel lumped-element coplanar waveguide-to-coplanar stripline transitions with low-pass and high-pass characteristics," in *IEEE MTT-S Int. Microwave Symp. Dig.*, pp. 2213-2216, 2002.

[7] Y.-S. Lin and C. H. Chen, "Coplanar waveguide-to-coplanar stripline transition-filter structures," in *2002 Asia-Pacific Microwave Conference Proceedings*, pp. 1489-1492.

[8] M. Ribo and L. Pradell, "Circuit model for a coplanar-slotline cross," *IEEE Microwave Guided Wave Lett.*, vol. 10, pp. 511-513, Dec. 2000.

[9] Y.-S. Lin and C. H. Chen, "Lumped-element impedance-transforming uniplanar transitions and their antenna applications" *IEEE Trans. Microwave Theory Tech.*, vol. 52, pp. 1157-1165, April 2004.